AJNR

Highlights of the scientific exhibits of the 29th annual meeting of the American Society of Neuroradiology, Washington, DC, June 9-14, 1991.

E J Russell

AJNR Am J Neuroradiol 1991, 12 (6) 1251-1257
http://www.ajnr.org/content/12/6/1251.citation

Highlights of the Scientific Exhibits of the 29th Annual Meeting of the American Society of Neuroradiology, Washington, DC, June 9–14, 1991

Eric J. Russell[1]

A total of 65 scientific exhibits were presented at the 29th annual meeting of the American Society of Neuroradiology (34 backboard panels and 24 view boxes). The display area was well attended throughout the meeting, a testament to the many high-quality exhibits. The following categorical summary provides a small sampling of the diverse material presented. It is meant to provide a review of new material presented in exhibit format, for those who had a limited time at the meeting and for those who could not attend.

Brain Neoplasms

Two exhibits covered selected MR characteristics of cerebral astrocytoma. Krol et al. examined the MR characteristics of 25 surgically proved anaplastic astrocytomas. A wide range of MR appearances was seen. Nine of the 25 cases showed no appreciable enhancement with contrast material, and 11 showed moderate or marked enhancement. The authors' findings reinforced previous studies that showed that an aggressive neoplasm may be present even when MR features otherwise appear benign.

Lefkowitz et al. examined the role of MR imaging in the evaluation of glioma recurrence. They found that the diagnosis of recurrent tumor was complicated by the coexistence of anatomic changes due to radiation therapy and surgical manipulation. Positron emission tomography (PET) data were also available in nine patients with previously treated glioma. Using metabolic activity and subsequent clinical course as gold standards, the authors gained insight into the pitfalls of MR interpretation in this patient group. When MR findings indicated improvement or stability in relation to the baseline appearance, PET activity was hypometabolic, leading the authors to conclude that MR can be used to reliably predict the absence of tumor recurrence in the early postoperative period. However, apparent progression of MR abnormalities was often misleading, as subsequent clinical follow-up did not show residual tumor in some of these cases.

A study by Alger et al. compared information gained by using ^{1}H spectroscopy or ^{18}F-fluoro-deoxyglucose PET in more than 50 cases of glioma. The authors found a lack of correlation between PET and MR spectroscopic studies, reflecting the different metabolic parameters measured. An increase in the rate of glucose utilization (indicated by hypermetabolic activity on PET) does not necessarily lead to accumulation of lactate (measured by MR spectroscopy). Lactate may dissipate despite its overproduction in active tumors. The authors indicated the need for further study to determine the significance of lactate as an independent measure of tumor growth. They also indicated that a decrease in n-acetyl aspartate and an increase in choline may be better MR spectroscopic markers for the presence of tumor than is lactate accumulation.

Cerebral Vascular Disease

Moody et al. presented an interesting exhibit to support their scientific paper on the prevalence of brain microemboli after cardiopulmonary bypass (CPB) surgery. They noted that at least 24% of the patients who have CPB have persistent neurologic deficits, and some have moderate to severe intellectual dysfunction. Moody et al. studied the brain microvasculature in five humans and six dogs after CPB. They found ubiquitous microvascular changes, including focal small capillary and arterial dilatations (SCADS) and microaneurysms. They theorized that these most likely were due to gas or oil emboli that were not directly seen in their anatomic preparations. No such abnormalities were found in 40 brains of subjects that did not have CPB. It is estimated that 15.3×10^{6} emboli were present in each case. Pathologic sections from the brains of patients who died shortly after cardiac surgery showed these changes and also showed unexplained birefringence, presumed to be a marker for SCADS (Fig. 1).

Below et al. reported on the neurologic complications of orthotopic liver transplantation. A retrospective review of medical records of 60 adults and children provided 17 cases in which the patients had significant postoperative neurologic abnormalities and neuroimaging correlations (emergency CT scans). Only two of 17 had normal CT scans. Hemorrhagic and ischemic complications were the most common finding, usually in patients who had postoperative seizures. The clinical significance of these sequelae was indicated by the fact that in 40%, these complications altered the patients' subsequent hospital course.

Ahmadi et al. described the MR characteristics of histopathologically complex cerebral vascular malformations. These complex angiomas may consist of side-by-side venous angioma and cavernous angioma (I have seen several cases of classic venous angioma adjacent to a lesion with MR characteristics typical of cavernous angioma). As selective

[1] Northwestern Memorial Hospital, Olson Pavilion, Ste. 3420, 710 N. Fairbanks Ct., Chicago, IL 60611.

AJNR 12:1251–1257, November/December 1991 0195–6108/91/1206–1251

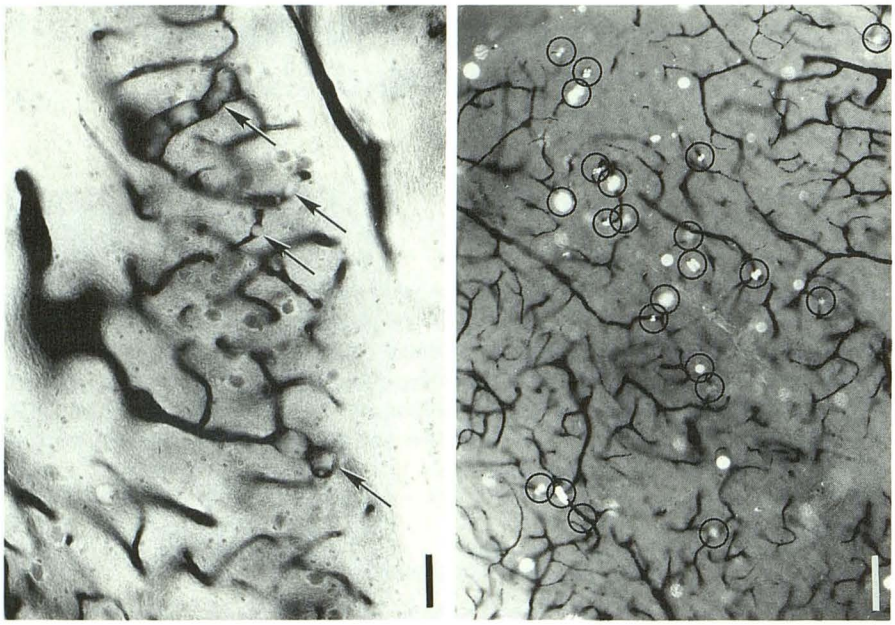

Fig. 1.—Thick (100-μm) celloidin sections of brains from patients who died shortly after cardiac surgery. Microvascular endothelium was stained for alkaline phosphatase.

A, Inferior olivary nucleus: *arrows* indicate two groups of three arteriolar small capillary and arterial dilatations (SCADs) (*right* and *left*) and two single SCADs in capillaries (*center*). Bar = 50 μm.

B, Caudate nucleus, in polarized light: SCADs often show an unexplained birefringence, which helps to locate them quickly and also shows sometimes heavy brain load. The 23 *circled* bright dots in this field proved to be SCADs on closer examination; remainder were unrelated particles. Bar = 25 μm.

surgical extirpation may spare normal local venous drainage, surgery may be altered if coexisting lesions are recognized beforehand.

Atrophy and White Matter Disease

An update of the data collected by the radiologic section of the Consortium to Establish a Registry for Alzheimer's Disease was presented by Davis et al. They found that interobserver ratings of atrophy and white matter lesions and infarcts were less than satisfactory despite the use of a standardized guidebook and data-reporting technique for grading MR images. Their findings suggest that a more objective semiautomated method of volumetric analysis may be needed for the comparison and pooling of MR data from multiple centers.

Edwards et al. reviewed the MR characteristics of Creutzfeldt-Jakob disease in 11 patients. Autopsy findings were available for five and biopsy results for three. This is a rare disease, primarily of white matter, characterized by progressive mental deterioration in middle-aged and elderly patients. Clinical onset is typically gradual, although it tends to be more rapidly progressive than that seen in Alzheimer disease. All patients with Creutzfeldt-Jakob disease had abnormal MR studies. The most common finding was atrophy. Other findings were subcortical white matter lesions, basal ganglionic lesions, and thinning of cortical gray matter. These MR features correlated with the pathologic findings of neuronal loss and gliosis in the cerebral cortex, basal ganglia, and subcortical white matter. The MR appearance of gray matter thinning in association with subcortical white matter abnormalities may suggest the diagnosis. Other findings were similar to those of other diffuse dementing processes.

Caldemeyer et al. reviewed the MR findings of acute disseminated encephalomyelitis in 12 patients. The age range was 12 months to 32 years. Focal neurologic findings were present in 11. Ten had an infectious disease 2 to 4 weeks before the onset of neurologic symptoms and signs. MR studies were abnormal in all 12 cases. CT studies (obtained in seven) were normal in six. All 10 patients with cerebral parenchymal abnormalities had multifocal white matter lesions with increased T2 relaxation times. Lesions were most common in periventricular and subcortical white matter, the brachium pontis, and the brainstem. Four patients had gray matter lesions. No hemorrhage or mass effect was observed. Three of five patients who received gadopentetate dimeglumine showed enhancement of lesions previously detected on T2-weighted images; thus, no lesions would have been missed if contrast material had not been used. One patient with optic neuritis had increased signal intensity within the optic nerve on short TI inversion recovery images. Follow-up MR showed a decrease in the size and number of white matter lesions, with complete resolution of many areas of presumed demyelination. Improved appearance on MR paralleled the course of clinical improvement.

Head Trauma

Orrison et al. conducted a review of 125 consecutive emergency department patients who had ultra–low-field-strength MR and concurrent CT examinations within 48 hr. These studies were read independently and randomly by two neuroradiologists who had no knowledge of the patients' histories. The positive predictive value of MR was higher than that of CT for the evaluation of contusions and subdural and epidural hematomas. However, the authors found that surgical management was altered because of the MR findings in only one of 125 cases, a case of unsuspected neoplasm. The study therefore supports the use of CT as the initial screening

study in patients who are neurologically impaired after head trauma.

Infection

Two outstanding exhibits dealt with neurocysticercosis. The first by Zee et al. was on the natural history of untreated cysticercosis. The authors were able to follow the evolution of the disease in 115 patients. MR images typically were available over 3–6 months (range, 4 weeks to 4 years).

Of 92 patients with cerebral parenchymal cysts, in 12%, new cysts developed or the size of previously detected cysts increased. A decrease in size of any or all cysts or complete resolution of any or all cysts was seen in 52 patients. No change was observed in 16 (17%). Therefore, in the majority of patients with parenchymal cysts (74%), the cysts evolved into a subsequent developmental stage, often accompanied by decreases in size or resolution of lesions on follow-up images.

Of three patients with spinal cysticercus cysts, spinal arachnoiditis developed in two who did not have intercurrent therapy. One such case is illustrated (Fig. 2).

One particularly interesting subset in the study was patients with intraventricular cysts (N = 27). Sixteen of these patients with hydrocephalus were treated with shunt placement only. Twelve of the 16 had serial images showing spontaneous cyst regression. Of the four patients who initially did not have shunts placed, one later needed surgery, but three had cyst regression without intervention. This study casts some doubt on the need for routinely aggressive medical therapy.

A beautiful compilation of the imaging and neuropathologic findings in cysticercosis was presented by Silva et al. Findings were based on cranial CT studies performed in 6298 cases over a 5-year period. The increased conspicuity of intraventricular cysts with MR imaging was clearly shown (Fig. 3). A particularly striking image in the exhibit was a scanning electron micrograph of the in vitro evagination of a *Taenia solium* cysticercus (Fig. 4).

Pediatrics

Blaser et al. correlated neuroimaging studies and clinical course in 100 children (average age, 3–6 years) with dural sinus/venous thrombosis. It is evident that sinovenous occlusive disease remains a difficult clinical diagnosis. The onset of seizures or hemiparesis in the context of hematologic disorder, trauma, or intracranial sepsis suggests the diagnosis. Ultimate prognosis depended more on the outcome of the underlying pathologic process than on that of the vascular thrombosis. Only 35 of 100 children were neurologically normal at follow-up. Fifteen children died from the underlying primary disease process, 13 died as a direct result of venous thrombosis. Radiologic findings included the classic delta sign of sagittal sinus thrombosis, tentorial enhancement, visualization of collateral veins, and hemorrhagic white matter infarction.

Castillo et al. summarized the MR and CT findings in eight patients with Chiari III malformations. All patients had high cervical/low occipital encephaloceles containing various amounts of brain. Sagittal MR studies were most helpful in detecting herniated tissue, and therefore in planning operative intervention. Common associated anomalies were dysgenesis of the corpus collosum (75%) and anomalous dural sinus and deep venous drainage (50%). Imaging analysis of local anomalous venous drainage is important so injury can be avoided during operative repair.

Ho et al. illustrated the differential diagnosis of bilateral basal ganglionic lesions in children. Acute causes included hypoxia, lactic acidosis, hypoglycemia, and central and extrapontine myelinolysis (Fig. 5). Chronic causes included inborn errors of metabolism, such as Leigh and Wilson diseases. Asymptomatic bilateral basal ganglionic processes included lesions associated with neurofibromatosis.

Spine

Several excellent exhibits were on spinal disease. Most dealt with MR imaging. However, one that did not provided information that answered a question many of us have often

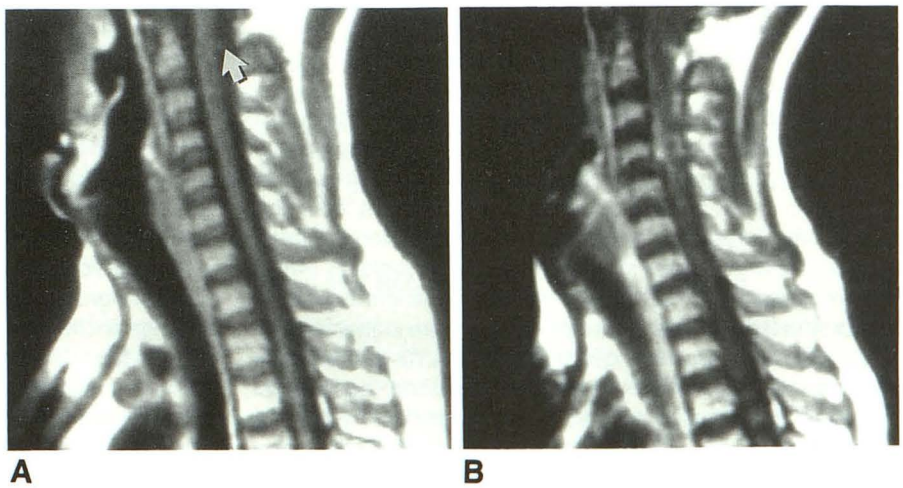

Fig. 2.—Spinal cysticercosis: Stage evolution without therapy.

A, Precontrast sagittal T1-weighted MR image shows scolex (*arrow*) in subarachnoid space dorsal to C2 level of spinal cord.

B, Postcontrast image obtained 5 months after A shows leptomeningeal enhancement on ventral and dorsal surfaces of cord. This sign of reactive inflammation represents cyst death and involution, a natural progression of disease.

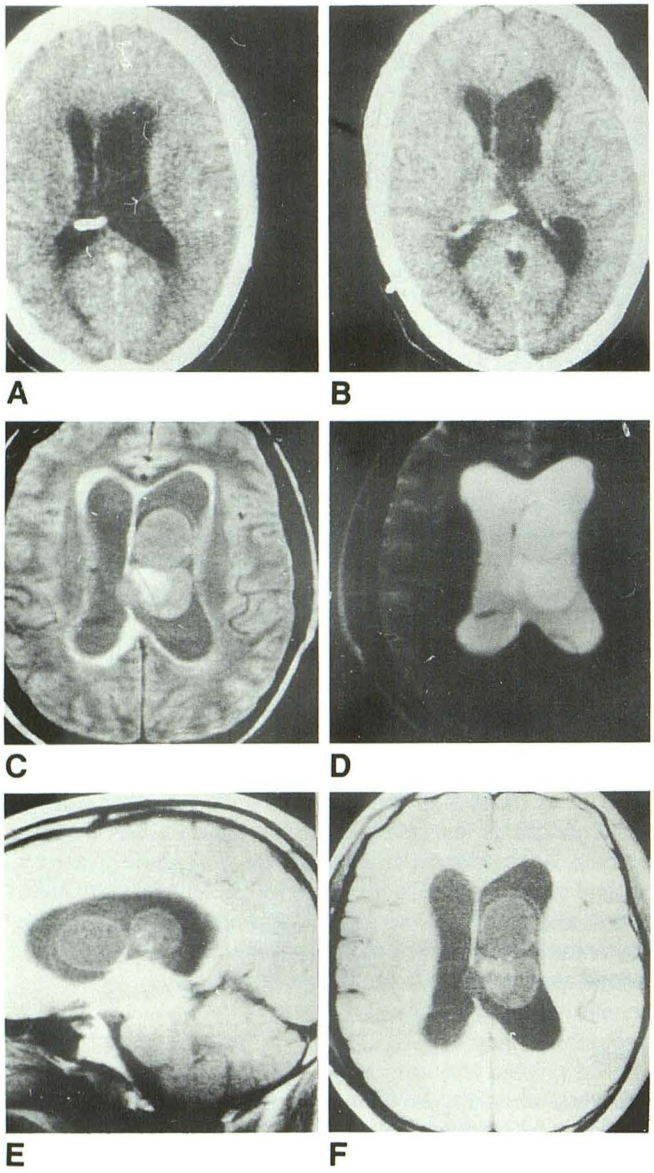

Fig. 3.—*A-E*, Intraventricular cysticercosis. Contrast-enhanced CT scans (*A*, *B*) and proton-density (*C*), T2-weighted (*D*), and T1-weighted (*E*, *F*) MR images show marked improvement in visualization of lateral ventricular cysticercus with MR.

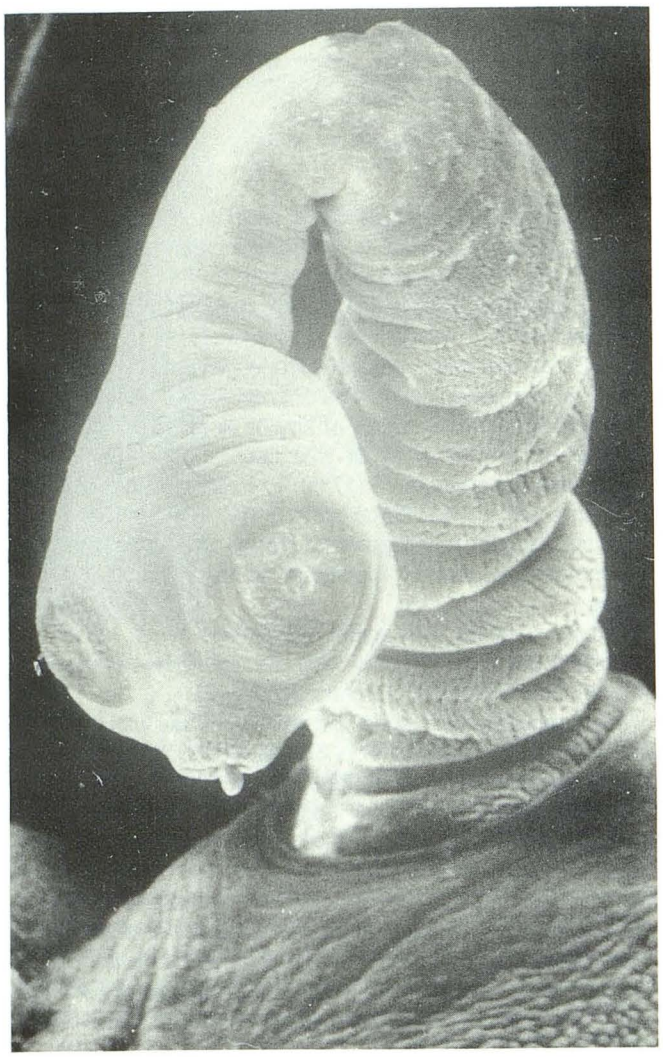

Fig. 4.—Scanning electron micrograph shows in vitro evagination of a *Taenia solium* cysticercus.

wondered about. Greiner et al. angiographically investigated 25 patients with blunt cervical spine trauma to determine the prevalence of traumatic injury to the vertebral arteries. Only those with midcervical subluxations or fractures coursing through the foramen transversarium were studied (bilateral vertebral artery injections). Twelve of these patients (48%) had significant vertebral artery injuries. Complete occlusion of the vertebral artery was detected in nine patients, and intimal disruption was found in three (Fig. 6). All nine patients with complete occlusion had no symptoms and received no treatment. Follow-up angiography in two patients who had incomplete lesions showed healing, with subtotal resolution at 3 and 6 weeks after treatment with heparin or aspirin. The third patient, who had dissection of the vertebral artery, was treated with low-dose heparin, but complete occlusion developed 2 days aftery injury (Fig. 6). None of these patients became symptomatic at any point. These findings are testaments to the natural protection provided by duplication of the vertebral artery system. As for the need to document such findings in asymptomatic patients, an interesting contrast can be made with the use of angiography for penetrating injuries of the neck. At my institution, angiography occasionally is ordered by the trauma service for patients with penetrating trauma to the neck between the angle of the mandible and the thoracic inlet (zone II), despite the absence of any major clinical signs (such as pulse deficit, expanding hematoma, or change in neurologic status). Such studies apparently are justified by wound proximity alone. The radiologic literature indicates an extraordinarily low yield of symptomatic arterial injury in this setting. Given the low but finite neurologic risk of emergency cerebral angiography, might it not be wise to withhold angiography in both clinical circumstances?

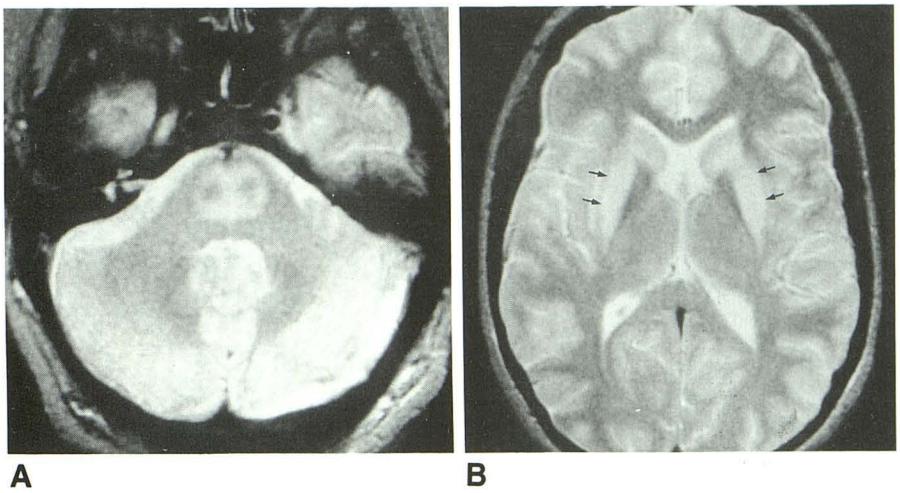

Fig. 5.—*A* and *B*, Extrapontine and pontine myelinolysis, a complication of rapid correction of sodium imbalance. T2-weighted MR images of brain of adolescent with spastic quadriparesis and pseudobulbar palsy that progressed in 5 days to "locked-in" syndrome show classic hyperintense demyelination in central pons (*A*) and associated abnormalities in both basal ganglia (*arrows*, *B*).

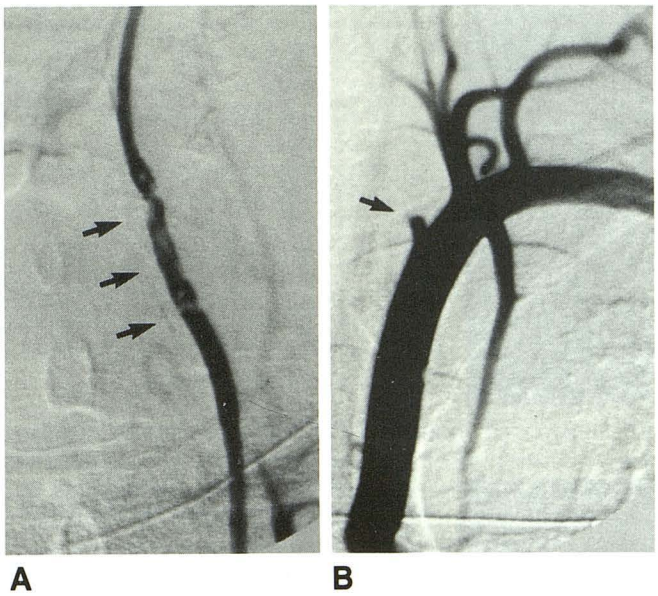

Fig. 6.—Arterial complication of midcervical dislocation.
***A*, Selective left vertebral angiogram obtained after left C5 articular dislocation and rotary subluxation at C5–C6 shows irregularity (*arrows*) of arterial lumen, representing dissection.**
***B*, Follow-up angiogram obtained 2 days after *A*, after low-dose heparin therapy, shows complete occlusion of artery with residual stump (*arrow*). Patient remained neurologically intact throughout.**

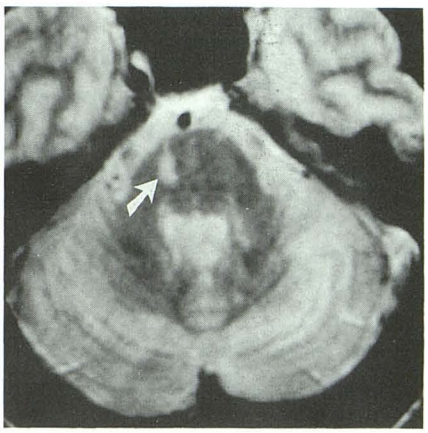

Fig. 7.—Infarction of right pons in patient with Raymond syndrome. Proton-density-weighted spin-echo MR image shows linear infarction in right pons (*arrow*) in a 76-year-old man with a right VI nerve palsy and contralateral hemiplegia. Lesion affects right corticospinal tract and tract of abducens (VI) nerve.

One popular exhibit, by Hahn et al. proposed the use of an additional cervicothoracic localizer (sagittal) scout image for MR imaging of the lumbosacral spine. This image would then be used as a "counting film" so that any transitional lumbar segments could be properly numbered. To obtain the scout image, the authors used the body coil on a GE 1.5-T scanner with 4.6 release software.

An extensive review of the clinical applications of MR imaging of spinal cord and CSF motion (350 cases) was provided by Levy et al. Pulsatile motion of spinal cord and CSF was evaluated by using cardiac-gated MR phase, cine, and tagging techniques. The authors reported that MR motion indexes correlated with symptomatic spinal cord compression and tethering and with clinical improvement observed postoperatively. For the determination of spinal cord motion, the size of the phase shift was displayed on a gray scale, with the amount of phase shift proportional to flow velocity along the frequency-encoding axis. Phase-contrast cinetechniques involved the subtraction of two interleaved gradient echo acquisitions, one with and one without flow compensation.

The authors reported that in cases of cord compression, static MR imaging may not correlate with the pre- or postoperative clinical picture. Motion images may be better for indicating the true status of the spinal cord. The authors noted good recovery of spinal cord motion and CSF flow postoperatively in patients with good clinical recovery after decompression of the upper cervical spine and foramen magnum, in a group of patients with achondroplasia.

Head and Neck

Two truly exceptional exhibits attracted much traffic during the meeting. One, by Laine et al., correlated the physiologic, anatomic, and imaging findings in cases of pathologic changes affecting the third, fourth, and sixth cranial nerves. Figures provided an illustrated review of the normal anatomic neuropathways from the brainstem to the orbit. Many clinical ex-

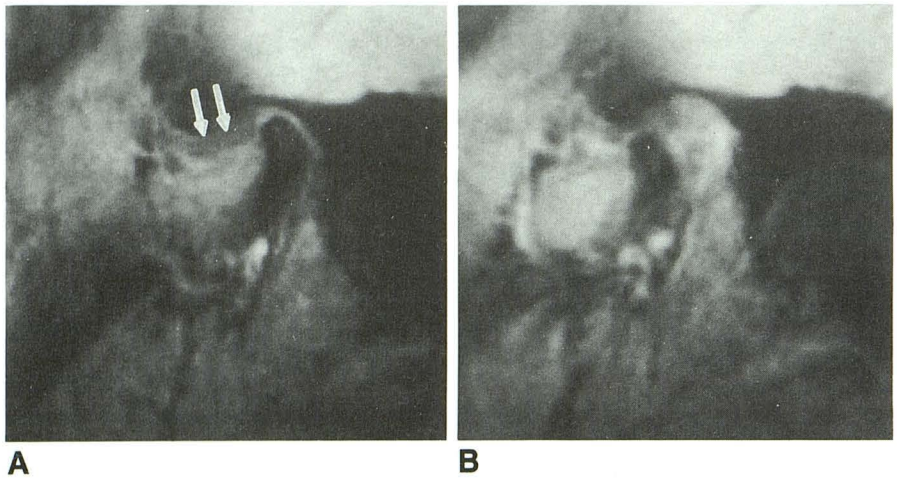

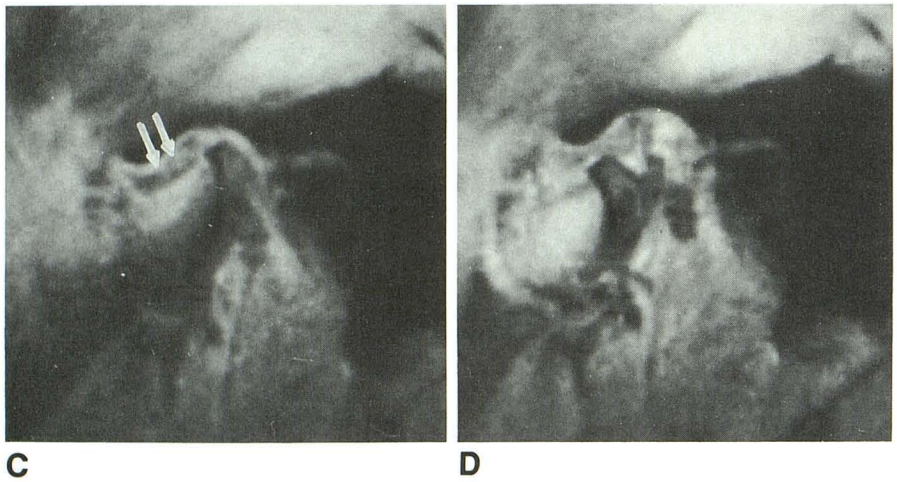

Fig. 8.—Failed meniscoplasty. *A–D*, Preoperative (*A*, *B*) and postoperative (*C*, *D*) sagittal open- and closed-mouth views of temporomandibular joint in patient with anteriorly dislocated disk (*double arrows*) show failure of improvement after surgery (*C*, *D*). Also, no improvement was seen in clinical symptom complex.

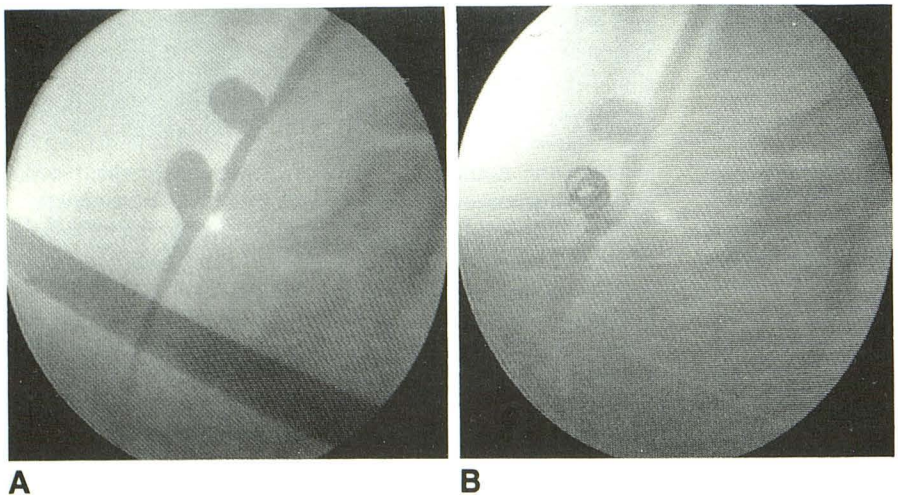

Fig. 9.—Laser-activated detachable coil device for aneurysm occlusion, experimental results.

***A*, Angiogram shows experimentally created venous patch aneurysm on common carotid artery of 20-kg mongrel dog.**

***B*, Angiogram obtained after deposition of coil shows occlusion of aneurysm dome.**

amples of patients with isolated and complex nerve palsies were presented, including an example of isolated abducens (VI) nerve palsy (Fig. 7). T2-weighted MR images in this patient with a right sixth nerve palsy and contralateral hemiplegia (Raymond syndrome) showed a focal area of infarction within the right pons affecting the corticospinal tract and the tract of the abducens nerve.

A well-organized exhibit by Conway et al. examined the postoperative MR findings in 20 patients with temporomandibular joint dysfunction after meniscoplasty. All patients had preoperative MR images that showed anterior dislocation of the disk, and all had standard meniscoplasty, with follow-up MR studies at an average of 6 months postsurgery. All 10 patients clinically graded as having excellent or good postoperative results had postoperative MR studies that showed the position of the disk was improved or normal. Fifteen

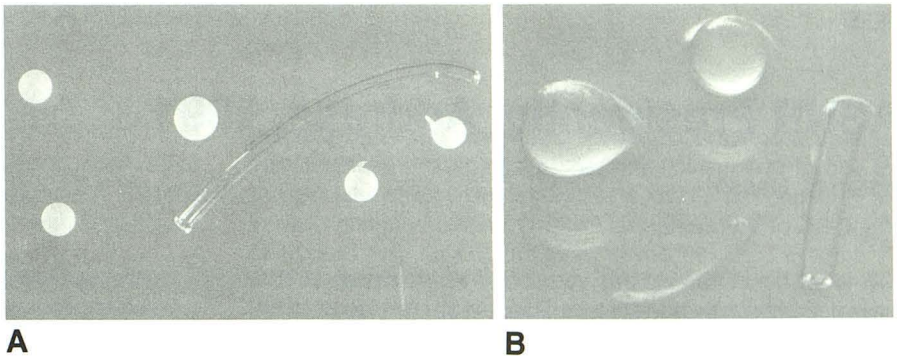

Fig. 10.—*A* and *B*, Hydrogel arterial beads and formed stents before (*A*) and after (*B*) hydration. Note swelling of all products after hydration (*B*).

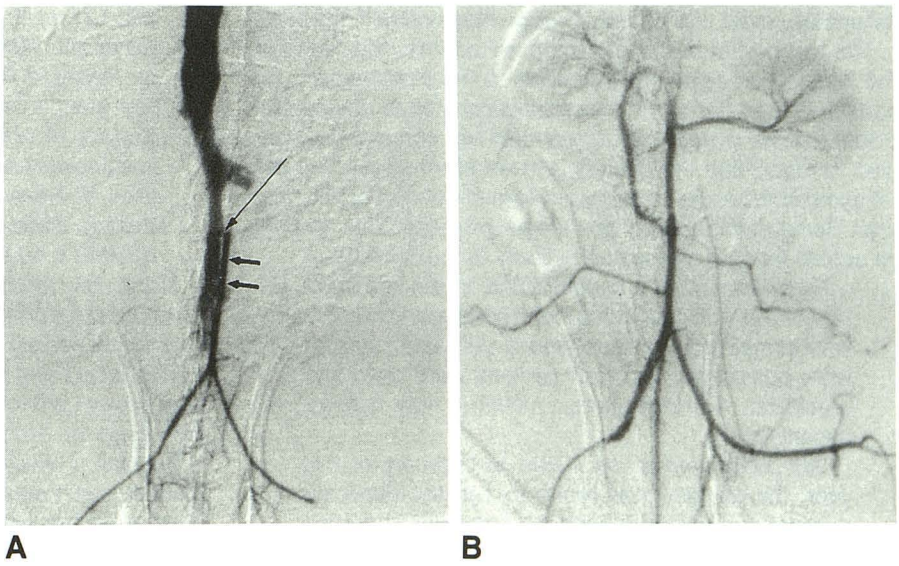

Fig. 11.—Stent therapy.
A, Pretreatment angiogram (*short arrows* point to aorta) in animal with experimental aortocaval fistula (*long arrow*).
B, Posttreatment aortogram. Hydrogel stent was placed in parent artery across fistula site, preserving aortic lumen.

patients, clinically classified as having fair or poor results, had MR studies that showed persistent anterior dislocation, with no improvement compared with preoperative images (Fig. 8). The authors cautioned that the results might depend on the type of surgery performed and that before these findings are applied, individual institutions should do their own pilot studies.

Interventional Neuroradiology

Numaguchi et al. presented an exhibit on the experimental use of ethylene vinyl alcohol (EVAL), a nonadhesive embolic agent developed by Taki in Japan. This material is a copolymer of EVAL, combined with dimethyl sulfoxide (DMSO) and metrizamide. The authors found the material too viscous to easily inject through a 2-French catheter and therefore diluted the EVAL mixture 1:2 with DMSO. The material is radiopaque, polymerizes in blood, and appears to be biocompatible. Histologic studies showed little reactive inflammation. Injection of the renal artery in rabbits was used to provide material for the histologic analysis. Further studies seem appropriate with this promising embolic agent.

Geremia et al. presented their investigational work with a laser-activated detachable coil meant to permit controlled detachment within aneurysms and other vascular lesions. Steel and platinum embolization coils are attached with heat-sensitive glue to quartz-fiber laser probes with diameters similar to that of the coils. Coil detachment is effected by laser activation. Artificially created aneurysms, made by attaching a jugular vein graft to the common carotid artery, were successfully treated (Fig. 9). This device is a variation of a similar system (nonlaser) principally investigated at UCLA Medical Center, which uses an electrically activated detachable coil. Preliminary clinical results with the UCLA device appear to indicate improved efficacy and safety when compared with currently available coils and balloons. The advantage of these devices compared with conventionally delivered embolic coils is the operator's ability to withdraw improperly positioned coils before final placement. Repeated introductions can be made until an optimal position is found.

The potential for the use of arterial stents within the cranial circulation was illustrated by preliminary work by Mehta et al. The authors have investigated the use of hydrogel, a soft hydrophilic material that can be shaped to create hollow vascular stenting devices. It is hoped that such devices may be flexible enough to permit delivery intracranially, with the goal of obstructing the orifices of aneurysms and fistulas without the necessity of sacrificing parent arteries. These materials enlarge when hydrated (Fig. 10), allowing treatment of arteries larger than the introducing device. I think that this may be potentially problematic, as swelling of the hydrogel might result in narrowing of the residual stent lumen. Laboratory studies in 10 rats with surgically created aortocaval fistulas showed successful treatment by placement of these devices in the inferior vena cava, or aorta, across the fistula site (Fig. 11).